

PLUTON EMPLACEMENT BY SHEETING AND VERTICAL BALLOONING
IN PART OF THE
SOUTHEAST COAST PLUTONIC COMPLEX,
BRITISH COLUMBIA

E. H. Brown and W.C. McClelland

DATA REPOSITORY

Procedures

Thermobarometry

Crystallization temperatures of the plutons (DR Table 1) were derived from compositions of coexisting plagioclase and hornblende utilizing the calibration of Holland and Blundy (1994). Barometry of the plutons is based on Al-in-hornblende, for which we used the calibration of Anderson and Smith (1995) which combines experimental work of Johnson and Rutherford (1989) and Schmidt (1992) to yield a pressure determination based both on the aluminum content of hornblende and the Holland and Blundy (1994) temperature of crystallization. The samples of this study are not ideal in the sense that many lack K-feldspar and sphene, suggested by some to be necessary phases in a pressure-buffering assemblage (e.g. Hollister and others, 1987). However, the temperature correction probably alleviates some degree of freedom of the incomplete assemblage. Furthermore, two observations suggest validity of the results: samples containing K-feldspar do not give significantly different results from those that lack this phase in the same area, and pressures determined for aureoles using garnet-aluminum silicate barometry (see below) correspond closely with Al-in-hornblende pressure from the adjacent pluton.

Thermobarometry of schists (DR Table 1) was determined from mineral equilibria: garnet+aluminum silicate+biotite+plagioclase+quartz or garnet+muscovite+biotite+plagioclase+quartz. The results are based on rim or near rim compositions of zoned minerals, and represent maximum recorded prograde conditions. Comparing results on replicate samples from the same or nearby outcrops, uncertainties due to mineral heterogeneity and analytical error are within ± 1.0 kbar and 50° C. Pressure-temperature calibration of the mineral equilibria is based on Berman (1991), using solution models as follows: garnet, Berman (1990); biotite, McMullin and others (1991), plagioclase, Fuhrman and Lindsley (1988).

U-Pb Geochronology

U-Pb zircon analyses were performed on 11 samples of plutons (Fig. 3; DR Table 2). Analytical procedures are outlined in McClelland and Mattinson (1996). The general rationale and basic techniques of the partial dissolution experiments are outlined by Mattinson (1994) and McClelland and Mattinson (1996). Error assignment for individual analyses follows Mattinson (1987) and is consistent with Ludwig (1992). Calculated $^{207}\text{Pb}/^{206}\text{Pb}$ and $^{206}\text{Pb}/^{238}\text{U}$ ratios incorporate a Th correction for potential deficit of radiogenic ^{206}Pb induced by exclusion of ^{230}Th during zircon crystallization (Mattinson, 1973; Schärer, 1984; Parrish, 1990). For this study, a $75\% \pm 25\%$ efficiency in ^{230}Th exclusion during zircon crystallization has been assumed.

Geology of the Plutons

Clear Creek Orthogneiss

The pluton termed here the Clear Creek Orthogneiss (published Fig. 4) was previously named the Hornet Creek Gneiss (Journeay and Friedman, 1993). It is renamed here because the body is centered on the Clear Creek drainage, and another pluton is prominent in the Hornet Creek drainage. A U-Pb zircon age of "ca. 226" Ma is reported by Monger (1989, analysis by van der Heyden). The protolith for the orthogneiss is tonalite (DR Fig. 2a). The rock is strongly gneissic, thoroughly recrystallized, and fairly homogenous. In the center of the body, at the core of the antiformal structure that folds the pluton, we observed an outcrop tens of meters across displaying a migmatitic injection complex of the orthogneiss into basic schist. This could represent the basal contact of the pluton and suggests intrusion of the pluton as an originally horizontal sheet. The southwestern contact of the Clear Creek Orthogneiss with the Cogburn terrane is intrusive, parallel to regional foliation, as evidenced by numerous sills of the orthogneiss in ribbon chert within 50 meters of the main orthogneiss body and xenoliths of schist within the orthogneiss sills.

Fir Creek pluton

The Fir Creek pluton was previously mapped by Reamsbottom (1971, 1974) as a metavolcanic rock in what he called the "Breakenridge Formation", wrapping the north end of the Breakenridge pluton. We interpret this body to be a sill based on intrusive contact relations, and separate it from the Breakenridge plutons based on its considerably older age (157.4 ± 0.5 Ma, DR Fig. 3a). The map extent shown to the north is based largely on Reamsbottom (1971). Three discordant zircon fractions indicate that this sample has experienced Pb-loss and contains inherited xenocrystic components of undetermined age. The Fir Creek pluton is contemporaneous with and is intruded into volcanic rocks of the Slollicum terrane and therefore probably represents a plutonic component of that terrane.

Settler Creek pluton

The Settler Creek pluton (published Fig. 4), is a small body with good magmatic textures and an aureole defined by pseudomorphed andalusite. An age of 96.7 ± 1.0 Ma is interpreted on the basis of two concordant zircon fractions (DR Fig. 3b).

Hut Creek pluton

The Hut Creek pluton (published Fig. 4) has magmatic textures, locally well-developed magmatic foliation, and a narrow aureole defined by sillimanite and pseudomorphed andalusite. Four concordant zircon fractions from this body indicate an age of 94.6 ± 0.5 Ma (DR Fig 3c).

Hornet Creek pluton

The Hornet Creek pluton (published Fig 3), newly named in this study, has magmatic textures throughout most of the body. The north and west sides of the Hornet Creek pluton have been overprinted by solid-state deformation that affects also the Breakenridge pluton. The pluton is not well mapped at the south end. An age of 98.3 ± 2 Ma is interpreted for this sample on the basis of a nearly concordant leach residue (DR Fig. 3d). Three discordant conventional zircon fractions from the Hornet Creek body indicate the presence of inherited xenocrystic components.

Breakenridge plutonic complex

Following Journeay and Friedman (1993), we use the name Breakenridge plutonic complex to include plutonic rocks in the core of the Breakenridge antiform and satellite sills in country rock up to several kilometers from the main body. This usage differs from that of Reamsbottom (1971, 1974) who used the term "Mount Breakenridge Complex" to refer to the

central pluton area only. He considered outlying sheets of gneiss to be of sedimentary and volcanic origin and included them in his "Breakenridge Formation"; however, our observation of homogenous textures, mafic inclusions, and intrusive contacts indicates a plutonic protolith.

Epizonal intrusion of the Breakenridge plutonic complex was suggested by Reamsbottom (1971) based on observation of porphyritic texture and miarolitic cavities in less deformed parts. Our finding of zoned garnet (published Fig. 3) with a core of low pressure origin (2-3 kilobars) in pelitic country rock at the southern BPC contact also suggests shallow intrusion.

Urquhart pluton

The rock body we have defined here as the Urquhart pluton (published Fig. 4) was mapped by Roddick and Hutchinson (1969) as part of the Spuzzum pluton. The present study shows that the pluton body in question is separated from the Scuzzy pluton to the north by a schist septum and has fabric concentric about a different center. Therefore we give this body a separate name, the Urquhart pluton, after Mount Urquhart, an impressive spire within the pluton.

Trajectories of magmatic foliations in the Urquhart pluton define a mostly concentric pattern in map view, parallel to the edge of the pluton and parallel also to metamorphic foliations in the strain aureole (published Fig. 4A). Foliation dips steeply inward on the north and east sides, and moderately inward (30 - 50°) on the west and south sides, parallel to the pluton contact in the vertical dimension as in plan view (published Fig. 4A; DR Fig. 5). Foliation is notably more strongly developed along the margins of the pluton than in the core. Foliations in the outer part of the pluton are interpreted to represent flow of crystal mush controlled by the pluton margin. Foliation in the southern part of the pluton core forms a macroscopic plunging syncline.

Magmatic lineation in the Urquhart pluton, defined primarily by aligned hornblende, is best developed along the west and south margins where it has a down-dip orientation, trending toward the pluton core (published Fig. 4B). Lineation is subvertical along the northern and eastern sides of the pluton. The marginal lineations are parallel to metamorphic mineral lineations in the inner strain aureole of the pluton (see below) and are reasonably interpreted to represent displacement direction of crystal-laden magma (e.g. Guillet and Bouchez, 1983; Cruden, 1990; Nicolas, 1992). In the core area, the magmatic lineation is mostly shallow, trending NW-SE, lying in steeply dipping foliation surfaces. This lineation could be interpreted to represent lateral flow of magma (e.g. Tobisch and Cruden, 1995), or alternatively tectonic deformation of crystal mush (e.g. Yoshinobu and Paterson, 1996), discussed below.

Local mafic hornblende-rich layers and felsic plagioclase-rich layers, one to several centimeters thick and traceable for a few meters, are apparently of magmatic origin. Fine-grained, dark dioritic inclusions, not highly strained, are readily found but are sparse.

The transition from country rock into the Urquhart pluton is characterized as follows: 1) First is a one to two kilometer wide injection/migmatite complex in which pelitic schists are host to a heterogeneous assemblage of mainly centimeter to meter thick felsic tonalite-granodiorite dikes and sills. 2) Next, is a sill complex a few hundred meters wide that consists of sheets of the distinctive Urquhart quartz diorite a few tens of meters thick alternating with screens of country rock ten or more meters thick. 3) Inward from the sill complex, the pluton is mostly continuous, but large concordant country rock screens occur locally along the western flank 2 to 3 kilometers from the pluton margin, suggesting that a significant thickness of the outer part of the pluton is sheeted. More than a few kilometers from the rim, the pluton is relatively homogeneous.

Crystallization temperatures of the Urquhart pluton, derived from coexisting plagioclase and hornblende (see above) are ~700° in a broad core area and 640° - 660° on the rim (DR Table 1). Along one transect at the western edge of the pluton, temperature measured in nine samples distributed over a distance of 2 kilometers increases continuously inward from 640° to 700°. Pressures throughout most of the pluton, based on Al-in-hornblende, are in the range of 5 to 6 kilobars (published Fig. 4B). Lower pressures, in the range of 3.8 to 4.3 kilobars, were measured along the western rim of the pluton; other parts of the rim give higher pressures, comparable to

those measured in the core. Confirmation that this variation of rim pressures is real comes from corresponding aureole pressures, described below.

Lineation patterns in the Urquhart aureole are complex. In a band next to the pluton, mostly one kilometer or less wide, weakly to moderately developed mineral lineation defined by andalusite (pseudomorphed) and sillimanite prisms plunges northeast, parallel to magmatic lineations in the adjacent pluton (published Fig 4B). Outside this belt, but still within the strain aureole, andalusite, sillimanite, and kyanite are weakly aligned northwest-southeast, at a high angle to lineations in the inner belt. Concordance of the lineations in the inner strain aureole with magmatic lineations in the rim of the pluton suggests that these represent the movement direction of magma at the contact of the pluton (as stated above).

We do not have a good explanation for the origin of the northwest trending lineations in the outer strain aureole. Possibilities are that they represent: 1) regional strain developed in the aureole due to thermal weakening, or 2) displacement of country rock parallel to movement of a sheet of magma some distance above. The northwest trending lineations in the outer strain aureole have approximately the same attitude as magmatic lineations in the core zone of the Urquhart pluton, the origin of which could be attributable to either lateral magmatic flow or regional tectonics (see above). Parallelism of the outer aureole lineations and the pluton core lineations suggests a common origin. Regional tectonics would seem to be the most likely process that could be common to both sets of structure. In support of this conclusion, NW-SE trending mineral and stretching lineations of the possibly coeval D4 regional tectonic event exist outside the Urquhart strain aureole. If this interpretation is correct, the regional strain must be considered to have been weak, not strong enough to cause solid-state deformation of the pluton as it cooled, or of the inner strain aureole of the country rock once it had crystallized under the influence of the marginal phase of the pluton.

Tikwalus Creek pluton

The Tikwalus Creek pluton is newly defined (published Fig. 4). This body is physically continuous with the Scuzzy pluton but can be distinguished based on composition and internal structure. The Tikwalus pluton consists of a complex of sills tens of meters thick separated by metamorphic screens. All planar structures, including magmatic fabric in the sills, metamorphic fabric in country rock, and intrusive contacts of the sills are nearly vertical and northwest striking. Details of the internal structure of the Tikwalus pluton have not been mapped. The fabric of this body strikes into and is cut off by the Scuzzy pluton. No U-Pb zircon age is available.

Big Silver pluton

The Big Silver pluton (published Fig. 3) was previously termed the Clear Creek Orthogneiss by Brown and Walker (1993), but is renamed here after its exposure in Big Silver Creek in light of further study because: 1) its fabric is not gneissic but magmatic and 2) the large Triassic orthogneiss body that dominates the upper Clear Creek drainage is more appropriately given this name. The Big Silver pluton is about 0.5 kilometers thick, and is more than 25 kilometers long, extending north outside the map area. This pluton is a composite of many rock types ranging from diorite to tonalite. The Big Silver pluton is a vertical dike intruded into, and slightly across, folded country rock terranes (published Fig. 2). A U-Pb zircon age of 91.4 ± 0.8 Ma was determined by Brown and Walker (1993) for rock at the south end of the body.

Mount Mason pluton

The Mount Mason pluton (published Fig. 3) is a large ovoid body (~10 X 30 kilometers) extending far beyond our study area to the northwest. A U-Pb zircon age of 91.5 ± 2 Ma was determined by Friedman and others (1992). Magmatic foliation is parallel to the contact at south end of the pluton, dipping 50-60 degrees under the pluton. Pronounced magmatic lineation has a down-dip orientation. A strain aureole less than one kilometer wide is indicated by deflection of regional structures. Sillimanite prisms in the strain aureole are parallel to magmatic lineation in the pluton.

Scuzzy pluton

Extending several kilometers out into country rock from the main body of the Scuzzy pluton, is an injection complex defined by pegmatite dikes and sills which comprise 10 to 50% of the country rock. Some of these bodies are tens of meters thick. Vein and layered migmatites (Mehnert, 1968) are intensely developed within a kilometer of the pluton.

Al-in-hornblende pressures in the outer zone of the Scuzzy pluton range from 4.4 - 7.7 kilobars, with the great majority being 5 - 5.5 kilobars (Fig 10). Plagioclase-hornblende temperatures are 700 to 750°C (DR Table 1).

U-Pb isotope partial dissolution results from the a northeastern rim sample (DR Fig. 3f) are similar to the results from the southwestern rim sample described in the published text (published Fig. 7c) but did not produce a concordant intermediate step. Thus, although similarities in zircon ages and systematics suggest the two rim samples are comparable in age, a precise age interpretation for the northeastern sample is not permissible. The interpreted age for the southwestern sample (89.8 ± 1.0 Ma) is consistent with an age of 87 ± 2 Ma interpreted from marginally concordant conventional fractions reported by Brown and Walker (1993, "Scuzzy Southwest").

Strain is manifest in Settler Schist by boudinaged and folded intrusive phases in the migmatitic border zone up to one kilometer from the Scuzzy pluton. Early formed andalusite porphyroblasts, now pseudomorphed by sillimanite, are in some places randomly oriented and in other places moderately aligned in a steep lineation. Foliation wraps the andalusite porphyroclasts and locally contains aligned sillimanite, but original shapes of andalusite grains are mostly preserved (DR Fig. 6B). On the northeast side of the pluton, meta-conglomerates show no relation of degree of strain to distance from the pluton and are inferred to have acquired their strain during earlier tectonic events; within one to two kilometers of the pluton, the meta-conglomerates and interbedded schists display mesoscopic secondary folds with a weak axial plane foliation (Alvarez, 1997).

References Cited

- Alvarez, K.M., 1997, Structure and metamorphism of the Kwoiek Creek area [M.S. thesis]: Western Washington University, Bellingham Washington, 141 p.
- Anderson, J.L. and Smith, D.R., 1995, The effect of temperature and oxygen fugacity on Al-in-hornblende barometry: *American Mineralogist*, v. 80, p. 549-559.
- Bennett, J.D., 1989, Timing and conditions of deformation and metamorphism of the structural packages east of Harrison Lake, B.C., [M.S. Thesis]: Bellingham, Western Washington University, 87p.
- Berman, R.G., 1990, Mixing properties of Ca-Mg-Fe-Mn garnets: *American Mineralogist*, v. 75, p. 328-344.
- Berman, R.G., 1991, Thermobarometry using multi-equilibrium calculations: a new technique, with petrologic applications: *Canadian Mineralogist*, v. 29, p. 833-855.
- Brown, E.H. and Burmester, R.F., 1991, Metamorphic evidence for tilt of the Spuzzum pluton: diminished basis for the "Baja British Columbia" concept: *Tectonics*, v. 10, p. 978-985.
- Brown, E.H. and Walker, N.W., 1993, A magma loading model for Barrovian metamorphism in the southeast Coast Plutonic Complex, British Columbia and Washington: *Geological Society of America Bulletin*, v. 105, p. 479-500.
- Cruden, A.R., 1990, Flow and fabric development during the diapiric rise of magma: *Journal of Geology*, v. 98, p. 681-698.
- Friedman, R.M., Tyson, T.M. and Journeay, J.M., 1992, U-Pb age of the Mt Mason pluton in the Cairn Needle area, southern Coast Belt, British Columbia: *Current Research, part A. Geological Survey of Canada*, v. Paper 92-1A, p. 261-266.

- Fuhrman, M.L. and Lindsley, D.H., 1988, Ternary feldspar modeling and thermometry: *American Mineralogist*, v. 73, p. 201-215.
- Guillet, P., Bouchez, J. and Vigneress, J.L., 1983, Anisotropy of magmatic susceptibility and magmatic structure in the Guerande granite massif (France): *Tectonics*, v. 2, p. 419-429.
- Holland, T.J.B. and Blundy, J.D., 1994, Non-ideal interactions in calcic amphiboles and their bearing on amphibole-plagioclase thermometry: *Contributions to Mineralogy and Petrology*, v. 116, p. 433-447.
- Hollister, L.S., Grissom, G.C., Peters, E.K., Stowell, H.H. and Sisson, V.B., 1987, Confirmation of the empirical correlation of Al in hornblende with pressure of solidification of calc-alkaline plutons: *American Mineralogist*, v. 72, p. 231-239.
- Johnson, M.C. and Rutherford, M.J., 1989, Experimental calibration of the aluminum-in-hornblende geobarometer with application to Long Valley caldera (California) volcanic rocks: *Geology*, v. 17, p. 837-841.
- Journeay, J.M. and Friedman, R.M., 1993, The Coast Belt thrust system: evidence of Late Cretaceous shortening in southwest British Columbia: *Tectonics*, v. 12, p. 756-775.
- Ludwig, K.R., 1992, Isoplot: A plotting and regression program for radiogenic-isotopic data, version 2.57: U.S. Geological Survey Open File Report 91-445.
- Mattinson, J.M., 1973, Anomalous isotope composition of lead in young zircons: *Carnegie Institution Yearbook* 72, p. 613-616.
- Mattinson, J.M., 1987, U-Pb ages of zircons: a basic examination of error propagation: *Chemical Geology*, v. 66, p. 151-162.
- Mattinson, J.M., 1994, A study of complex disorder in zircons using stepwise dissolution techniques: *Contributions to Mineralogy and Petrology*, v. 116, p. 117-129.
- McClelland, W.C. and Mattinson, J.M., 1996, Resolving high precision U-Pb ages from Tertiary plutons with complex zircon systematics: *Geochimica et Cosmochimica Acta*, v. 60, p. 3955-3965.
- McMullen, D.W., Berman, R.G. and Greenwood, H.J., 1991, Calibration of the SGAM thermobarometer for pelitic rocks using data from phase-equilibrium experiments and natural assemblages: *Canadian Mineralogist*, v. 29, p. 889-908.
- Mehnert, K.R., 1968, Migmatites and the origin of granitic rocks: Amsterdam, Elsevier, 393p.
- Monger, J.W.H., 1989, Geology of Hope and Ashcroft map areas, British Columbia, Maps 41-1989 and 42-1989, 1:250,000: Geological Survey of Canada.
- Parrish, R.R., 1990, U-Pb dating of monazite and its application to geological problems: *Canadian Journal of Earth Sciences*, v. 27, p. 1431-1450.
- Nicolas, A., 1992, Kinematics in magmatic rocks with special reference to gabbros: *Journal of Petrology*, v. 33, p. 891-915.
- Reamsbottom, S.B., 1971, The geology of the Mount Breakenridge area, Harrison Lake, B.C., [M.Sc. Thesis]: University of British Columbia, Vancouver, B.C., 162 p.
- Reamsbottom, S.B., 1974, Geology and metamorphism of the Mount Breakenridge area, Harrison Lake, British Columbia, [Ph.D. Thesis]: University of British Columbia, Vancouver, B.C., 155p.
- Roddick, J.A. and Hutchinson, W.W., 1969, Northwestern part of Hope map-area, British Columbia [92H (west half)]: Geological Survey of Canada Paper 69-1A, p. 29-38.
- Scharer, U., 1984, The effect of initial ^{230}Th disequilibrium in young U-Pb ages: the Makalu case, Himalaya: *Earth and Planetary Science Letters*, v. 67, p. 191-204.
- Schmidt, M.W., 1992, Amphibole composition in tonalite as a function of pressure: an experimental calibration of the Al-in-hornblende barometer: *Contributions to Mineralogy and Petrology*, v. 110, p. 304-310.
- Stacey, J.S. and Kramers, J.D., 1975, Approximation of terrestrial lead isotope evolution by a two-stage model: *Earth and Planetary Science Letters*, v. 26, p. 207-221.
- Tobisch, O.T. and Cruden, A.R., 1995, Fracture-controlled magma conduits in an obliquely convergent continental magmatic arc: *Geology*, v. 23, p. 941-944.
- Yoshinobu, A. and Paterson, S.R., 1996, Fracture-controlled magma conduits in an obliquely convergent continental magmatic arc: comment: *Geology*, v. 24, p. 669-670.

Figure Captions

DR Figure 1. Localities of thermobarometric samples listed in DR Table 1.

A. Samples in the vicinity of the Urquhart pluton.

B. Samples in the vicinity of the Scuzzy pluton.

DR Figure 2. Modal composition of plutons based on point count analyses of stained slabs, ~1000 points/sample. K-feldspar is in trace amount or absent in all samples except those shown on DR Fig 1B. Mafics are biotite and/or hornblende in most samples.

A. Quartz - plagioclase - mafics plot of sparsely sampled plutons.

B. Quartz - plagioclase - K-feldspar plot of the Breakenridge and Scuzzy plutons.

C. Quartz-plagioclase-mafics plot in abundantly sampled plutons. Numbers of samples: Scuzzy core 40, Scuzzy rim 41, Urquhart 98, Tikwalus Ck 37.

DR Figure 3. U-Pb concordia diagrams for dated samples. Analytical data presented in DR Table 2. See published paper and repository text for discussion.

DR Figure 4. Photo of outcrop-scale, sheeted injection complex of the Breakenridge Plutonic Complex. Light rock is tonalite, dark rock is diorite. This rock has solid-state fabric. Knife in the center of photo provides a scale.

DR Figure 5. Map trace across topography of the moderately inward dipping south contact of the Urquhart pluton.

A. Map of part of the south contact of the Urquhart pluton. Areas of pattern show observed outcrops. The attitude of the contact of the pluton determined from its trace across topography is similar to the attitude of magmatic and metamorphic foliations measured nearby in the pluton and country rock respectively. Contour interval is 500 feet.

B. Location map for DR 5A.

DR Figure 6. Early contact metamorphic andalusite, now pseudomorphed by sillimanite.

A. View on foliation surface of randomly oriented andalusite in the aureole of the Urquhart pluton. The andalusite post-dates the quartz rod lineation and provides evidence for relatively low strain during development of the Urquhart aureole. Hammer for scale.

B. Photomicrograph of pseudomorphed andalusite. View down c-axis. The andalusites are pseudomorphed by sillimanite such that a single crystal of andalusite is replaced by a topotactic, multi-crystal aggregate of sillimanite; the c-axes of a bundle of sillimanite needles are parallel to the original c-axis of andalusite. A faint relict chiastolite cross is preserved. Foliation wraps the andalusite. The original crystal form is well preserved, indicating an absence of strong penetrative strain subsequent to andalusite crystallization. This sample is from the aureole of the Scuzzy pluton.

DR Figure 7. Sheeted margin of the Scuzzy pluton in the vicinity of Big Silver Creek.

A. Detailed Map. Note: 1) outlying sill, composed of plutonic rock similar to that in the main body of the pluton, 2) zone of trains of country rock screens and pluton sheets within the main mass of the pluton. "PHOTO" gives the locality of the screen/sheet complex shown in Fig. 10 of the published paper. Foliation symbols as in Fig. 9 of the published paper.

B. Location of DR Fig. 7A.

DR Table 1 Compositions of Minerals used for Thermobarometry

Map Number	1				2			3				4		
Field Number	162-196				164-231			164-228				117-2		
Rock Unit	SL				SE			SE				SE		
Reference	4				2			1				1		
Mineral	GA	BI	MU	PL	GA	BI	PL	GA	BI	MU	PL	GA	BI	PL
Wt% Oxide SiO ₂	36.7	35.53	45.1	61.6				36.3	36.1	44.8	56.6	36.8	34.7	60.0
TiO ₂	0.00	1.48	0.5					0.05	1.58	0.56		0.03	2.39	
Al ₂ O ₃	20.9	18.2	35.0	24.08				20.7	17.9	32.9	24.7	21.1	19.3	25.0
FeO	33.0	19.8	1.20	0.09				30.5	17.4	0.94		33.2	18.5	
MnO	3.89	0.03	0.00					5.55	0.01	0.00		1.71	0.03	
MgO	2.74	9.88	0.70					2.73	11.9	0.74		4.06	10.4	
CaO	1.73			5.28				2.26			6.72	2.32		6.60
Na ₂ O		0.06	1.48	8.60					0.24	1.60	7.82		0.30	7.99
K ₂ O		9.06	8.51	0.05					8.07	8.5	0.06		8.67	0.06
Total	98.9	94.03	92.4	99.7				97.8	92.2	90.0	95.9	99.2	94.3	99.7
Cations Si	2.99	5.48	6.14	2.74	2.98	5.95		2.97	5.55	6.26	2.64	2.97	5.79	2.68
Ti	0.00	0.172	0.050			0.22		0.003	0.183	0.059			0.30	
Al	2.01	3.31	5.61	1.26	2.00	3.78		2.000	3.25	5.42	1.36	2.01	3.79	1.32
Fe	2.25	2.55	0.14	0.003	2.20	2.33		2.20	2.11	0.110		2.24	2.58	
Mn	0.269	0.004	0.00		0.03			0.062	0.001	0.000		0.11	0.003	
Mg	0.333	2.27	0.14		0.43	2.83		0.457	2.73	0.154		0.49	2.59	
Ca	0.151			0.252	0.40		0.34	0.347			0.336	0.21		0.316
Na		0.018	0.39	0.742		0.05	0.67		0.072	0.435	0.707		0.100	0.692
K		1.78	1.48	0.003		1.59			1.58	1.52	0.004		1.85	0.004
Temperature °C	575, GABI				603, GABI			613, GABI				625, GABI		
Pressure, kilobars	4.6, GAMI				7.9, GASP-Ky			7.7, GASP-Ky				7.1, GASP-Ky		

Table 1 Compositions of Minerals used for Thermobarometry

Map Number	5			6			7				8		
Field Number	164-233D			P3			179-MN31				164-258F		
Rock Unit	SE			SE			SE				SE		
Reference	2			5			1				2		
Mineral	GA	BI	PL	GA	BI	PL	GA	BI	MU	PL	GA	BI	PL
Wt% Oxide SiO ₂							37.2	36.8	50.3	61.2			
TiO ₂								1.58	0.40				
Al ₂ O ₃							20.6	19.3	38.8	24.4			
FeO							35.3	19.1	1.20	0.06			
MnO							0.55						
MgO							2.75	10.5	0.67				
CaO							2.97			5.59			
Na ₂ O								0.16	0.92	8.68			
K ₂ O								8.18	8.08	0.05			
Total							99.3	95.6	100.3	100.0			
Cations Si	3.00	5.86		2.95	5.44		3.01	5.50	6.22	2.72	2.97	5.80	
Ti		0.25			0.20			0.178	0.037			0.303	
Al	1.98	3.87		2.04	3.48		1.97	3.41	5.66	1.28	2.01	3.87	
Fe	2.22	2.27		2.24	2.15		2.39	2.39	0.12	0.002	2.20	2.51	
Mn	0.13	0.01		0.13			0.038				0.150	0.01	
Mg	0.48	2.77		0.43	2.50		0.332	2.34	0.12		0.500	2.56	
Ca	0.22		0.30	0.23			0.258			0.266	0.181		0.32
Na		0.10	0.70		0.07	0.32		0.046	0.221	0.747		0.05	0.68
K		1.77			1.67	0.70		1.56	1.276	0.003		1.74	
Temperature °C	591, GABI			584, GABI			558, GABI				661, GABI		
Pressure, kilobars	6.0, GASP-Ky			5.9, GASP-Ky			6.0, GAMI				6.4, GASP-Si		

Table 1 Compositions of Minerals used for Thermobarometry

Map Number		9			10		11		12		13		14	
Field Number		164-258H			164-259		179-AH19		164-435		179-AH23		179-AH35	
Rock Unit		SE			UP		UP		UP		UP		UP	
Reference		2			1,2		1		1,2		1		1	
Mineral		GA	BI	PL	HB	PL	HB	PL	HB	PL	HB	PL	HB	PL
Wt% Oxide	SiO ₂				44.4	60.2	43.2	57.7	47.3	60.1	45.7	57.9	46.9	58.5
	TiO ₂				1.14		1.08		1.17		1.09		1.08	
	Al ₂ O ₃				11.8	24.8	12.02	25.0	8.81	24.8	10.08	25.2	8.37	24.8
	FeO				15.6		15.73		14.3		15.7	0.06	16.0	
	MnO				0.34		0.33		0.37		0.44		0.43	
	MgO				12.2		10.97		12.5		11.7		12.0	
	CaO				11.0	6.73	11.02	6.66	11.8	6.85	10.6	6.97	10.9	6.56
	Na ₂ O				1.58	7.76	1.71	7.71	1.08	7.68	1.33	7.64	1.20	7.84
	K ₂ O				0.44	0.08	0.56	0.11	0.51	0.009	0.43	0.10	0.39	0.14
	Total				98.5	99.6	96.7	97.1	97.8	99.4	97.1	97.9	97.2	97.9
Cations	Si	3.00	5.86		6.37	2.69	6.41	2.65	6.87	2.69	6.71	2.64	6.90	2.67
	Ti		0.28		0.123		0.12		0.128		0.12		0.119	
	Al	2.01	3.88		1.99	1.31	2.10	1.35	1.51	1.31	1.75	1.35	1.45	1.33
	Fe ₃				1.131		0.596		0.383		0.530		0.475	
	Fe ₂	2.20	0.30		0.739		1.358		1.36		1.40	0.002	1.49	
	Mn	0.10	0.01		0.041		0.042		0.046		0.055		0.054	
	Mg	0.51	2.65		2.61		2.43		2.71		2.56		2.62	
	Ca	0.18		0.31	1.69	0.322	1.75	0.328	1.84	0.328	1.67	0.341	1.72	0.320
	Na		0.07	0.69	0.439	0.672	0.492	0.687	0.305	0.666	0.379	0.676	0.334	0.693
	K		1.84		0.080	0.005	0.106	0.006	0.095	0.001	0.081	0.006	0.073	0.008
Temperature °C		624, GABI			745, HBPL		717, HBPL		662, HBPL		683, HBPL		675, HBPL	
Pressure, kilobars		5.9, GASP-Si			5.3, ALHB		6.3, ALHB		4.29, ALHB		5.2, ALHB		3.9, ALHB	

Table 1 Compositions of Minerals used for Thermobarometry

Map Number	15			16			17			18			19	
Field Number	JT 88-05			162-192			164-460			179-NB125			179-NB132	
Rock Unit	SE			SE			SE			SE			UP	
Reference	2			2,4			1			1			1	
Mineral	GA	BI	PL	GA	BI	PL	GA	BI	PL	GA	BI	PL	HB	PL
Wt% Oxide SiO ₂							37.5	35.3	60.6	37.6	35.0	59.6	48.0	58.8
TiO ₂								1.82			2.26		1.01	
Al ₂ O ₃							21.2	18.9	24.7	21.4	18.1	25.1	8.23	25.5
FeO							33.6	17.25		32.8	16.9		15.2	
MnO							1.29	0.00		1.09	0.00		0.47	
MgO							4.48	11.0		5.21	11.1		12.4	
CaO							1.43		6.37	1.24		6.73	11.1	7.38
Na ₂ O								0.24	7.99		0.24	7.77	1.05	7.32
K ₂ O								8.63	0.06		9.18	0.13	0.40	0.12
Total							99.5	93.1	99.8	99.4	92.7	99.3	97.9	99.1
Cations Si	2.97	5.66		2.96	5.70		3.00	5.67	2.70	3.00	5.42	2.67	6.93	2.65
Ti		0.28			0.24			0.220			0.263		0.11	
Al	2.00	3.40		2.00	3.52		2.00	3.58	1.30	2.01	3.30	1.33	1.40	1.35
Fe ₃													0.72	
Fe ₂	2.19	2.48		2.20	2.25		2.25	2.32		2.19	2.19		1.12	
Mn	0.21	0.01		0.20	0.01		0.088			0.074			0.06	
Mg	0.52	2.58		0.42	2.70		0.535	2.63		0.619	2.55		2.67	
Ca	0.140		0.33	0.27		0.39	0.123		0.304	0.106		0.323	1.72	0.356
Na		0.05	0.67		0.06	0.62		0.074	0.690		0.072	0.676	0.29	0.639
K		1.85			1.69			1.77	0.003		1.81	0.007	0.07	0.007
Temperature, °C	667, GABI			572, GABI			632, GABI			684, GABI			652, HBPL	
Pressure, kilobars	5.0, GASP-Si			5.4, GASP-Ky			4.4, GASP-Si			4.4, GASP-Si			3.8, ALHB	

Table 1 Compositions of Minerals used for Thermobarometry

Map Number	20		21		22		23		24		25		26	
Field Number	179-NB123		179-NB120		176-137		176-209		176-115		176-116		176-119	
Rock Unit	UP		UP		UP		UP		UP		UP		UP	
Reference	1		1		1		1		1		1		1	
Mineral	HB	PL	HB	PL	HB	PL	HB	PL	HB	PL	HB	PL	HB	PL
Wt% Oxide SiO ₂	46.7	57.3	46.0	59.1	45.3	59.1	44.6	60.6	45.9	58.6	45.1	59.5	45.3	60.8
TiO ₂	0.93		0.65		0.88		0.93		0.81		0.82		0.87	
Al ₂ O ₃	9.92	26.5	10.6	25.5	11.5	25.9	11.2	24.6	11.7	26.1	11.5	25.4	11.0	24.7
FeO	15.9		16.2		15.9		16.0		14.3		16.1		15.8	
MnO	0.29		0.32		0.31		0.30		0.21		0.28		0.35	
MgO	12.4		12.0		12.0		11.5		12.5		12.0		11.3	
CaO	10.1	8.53	10.1	7.14	10.2	7.83	11.3	6.50	10.7	7.62	10.3	7.40	11.6	6.44
Na ₂ O	1.17	6.84	1.31	7.42	1.44	7.20	1.61	7.79	1.56	7.30	1.56	7.40	1.34	7.82
K ₂ O	0.33	0.12	0.32	0.12	0.31	0.11	0.57	0.14	0.27	0.06	0.34	0.08	0.68	0.23
Total	97.7	99.3	97.5	99.3	97.8	100.1	98.0	99.6	98.0	99.7	98.0	99.8	98.2	100.0
Cations Si	6.66	2.59	6.60	2.65	6.47	2.64	6.49	2.70	6.56	2.63	6.45	2.66	6.60	2.70
Ti	0.100		0.070		0.095		0.102		0.09		0.088		0.09	
Al	1.67	1.41	1.80	1.35	1.94	1.36	1.92	1.29	1.97	1.38	1.94	1.34	1.89	1.30
Fe ₃	1.35		1.34		1.35		0.798		1.00		1.33		0.60	
Fe ₂	0.55		0.601		0.555		1.15		0.71		0.601		1.32	
Mn	0.035		0.039		0.038		0.037		0.03		0.034		0.04	
Mg	2.63		2.56		2.56		2.50		2.66		2.56		2.45	
Ca	1.54	0.412	1.56	0.343	1.56	0.374	1.763	0.311	1.64	0.366	1.58	0.354	1.81	0.307
Na	0.32	0.598	0.364	0.646	0.399	0.622	0.455	0.674	0.43	0.634	0.421	0.641	0.38	0.674
K	0.060	0.007	0.059	0.007	0.057	0.006	0.106	0.008	0.05	0.003	0.062	0.004	0.13	0.013
Temperature °C	683, HBPL		673, HBPL		719, HBPL		714, HBPL		680, HBPL		718, HBPL		678, HBPL	
Pressure, kilobars	4.9, ALHB		5.5, ALHB		5.08, ALHB		5.6, ALHB		6.3, ALHB		5.6, ALHB		6.0, ALHB	

Table 1 Compositions of Minerals used for Thermobarometry

Map Number	27		28		29			30		31		32	
Field Number	176-129		176-125		179-CB1			176-211		176-212		176-217	
Rock Unit	UP		UP		SE			UP		UP		UP	
Reference	1		1		1			1		1		1	
Mineral	HB	PL	HB	PL	GA	BI	PL	HB	PL	HB	PL	HB	PL
Wt% Oxide													
SiO ₂	45.3	59.6	45.5	59.8	36.2	35.7	58.3	46.3	60.3	46.7	59.9	44.3	60.7
TiO ₂	0.93		0.88		0.04	2.44		0.81		0.76		1.00	
Al ₂ O ₃	11.4	25.1	11.3	25.1	20.1	19.2	26.1	10.9	25.1	9.98	25.2	11.00	24.6
FeO	15.1		15.2		36.7	18.9	0.04	15.5		15.2		15.8	
MnO	0.30		0.31		0.75	0.04		0.30		0.30		0.28	
MgO	12.2		11.7		2.18	10.3		12.3		12.6		11.7	
CaO	10.4	7.33	10.7	7.17	3.75		7.74	10.4	6.30	10.9	7.02	11.4	6.45
Na ₂ O	1.66	7.49	1.58	7.48		0.20	7.14	1.51	8.03	1.40	7.58	1.52	7.85
K ₂ O	0.30	0.11	0.31	0.16		8.58	0.05	0.29	0.06	0.33	0.07	0.69	0.13
Total	97.6	99.6	97.5	99.7	99.8	95.2	99.4	98.3	99.8	98.2	99.8	97.7	99.7
Cations													
Si	6.51	2.67	6.58	2.67	2.96	5.39	2.62	6.59	2.69	6.69	2.67	6.48	2.71
Ti	0.10		0.10		0.002	0.277	1.38	0.09		0.08		0.11	
Al	1.93	1.32	1.93	1.32	1.94	3.41		1.83	1.32	1.68	1.33	1.90	1.29
Fe ₃	1.13		0.90					1.17		0.98		0.79	
Fe ₂	0.68		0.94		2.51	2.38	0.002	0.68		0.84		1.14	
Mn	0.04		0.04		0.052	0.005		0.04		0.04		0.03	
Mg	2.61		2.52		0.266	2.31		2.61		2.69		2.55	
Ca	1.60	0.351	1.66	0.344	0.329		0.373	1.59	0.301	1.67	0.336	1.79	0.308
Na	0.46	0.650	0.44	0.649		0.059	0.622	0.42	0.693	0.39	0.656	0.43	0.678
K	0.05	0.006	0.06	0.009		1.65	0.003	0.05	0.003	0.06	0.004	0.13	0.007
Temperature °C	713, HBPL		685, HBPL		638, GABI			676, HBPL		689, HBPL		723, HBPL	
Pressure, kilobars	5.6, ALHB		6.1, ALHB		5.3, GASP-Si			5.7, ALHB		4.8, ALHB		5.3, ALHB	

Table 1 Compositions of Minerals used for Thermobarometry															
Map Number		33		34		35		36			37		38		
Field Number		176-215		176-124		164-196		179-NB55			176-220		JT89-17		
Rock Unit		UP		UP		SP		SE			SP		SE		
Reference		1		1		1,2		1			1		2		
Mineral		HB	PL	HB	PL	HB	PL	GA	BI	PL	HB	PL	GA	BI	PL
Wt% Oxide	SiO2	45.4	61.1	45.8	60.2	42.6	57.4	36.8	35.6	60.4	47.1	59.9			
	TiO2	0.79		1.12		1.05			2.68		0.94				
	Al2O3	10.3	24.6	10.2	24.9	11.5	25.0	20.6	19.3	25.3	8.83	25.0			
	FeO	16.2		15.8		18.7	0.04	34.0	18.9	0.05	15.3				
	MnO	0.27		0.36		0.49		3.61	0.04		0.38				
	MgO	11.7		11.5		9.54		4.08	10.5		12.1				
	CaO	11.4	6.40	11.6	6.69	11.5	6.77	1.77		6.94	11.5	6.90			
	Na2O	1.45	7.96	1.40	7.62	1.55	7.74		0.22	8.02	1.07	7.67			
	K2O	0.57	0.16	0.70	0.13	0.86	0.18		8.19	0.07	0.60	0.16			
	Total	98.1	100.2	98.5	99.5	97.8	97.1	100.9	95.4	100.7	97.9	99.6			
Cations	Si	6.61	2.71	6.67	2.69	6.35	2.64	2.95	5.36	2.67	6.85	2.68	2.99	5.63	
	Ti	0.09		0.12		0.12			0.303		0.10			0.30	
	Al	1.77	1.29	1.75	1.31	2.02	1.36	1.95	3.43	1.32	1.51	1.32	2.00	3.49	
	Fe3	0.78		0.53		0.76					0.59				
	Fe2	1.19		1.39		1.57	0.002	2.28	2.37	0.002	1.27		2.10	2.40	
	Mn	0.03		0.04		0.06		0.245	0.005		0.05		0.23	0.01	
	Mg	2.54		2.49		2.12		0.488	2.35		2.63		0.54	2.53	
	Ca	1.78	0.304	1.81	0.320	1.84	0.334	0.152		0.329	1.79	0.331	0.15		0.33
	Na	0.41	0.685	0.39	0.660	0.45	0.690		0.064	0.688	0.30	0.665		0.08	0.69
	K	0.11	0.009	0.13	0.007	0.16	0.011		1.57	0.004	0.11	0.009		1.75	
Temperature °C		702, HBPL		692, HBPL		742, HBPL		650, GABI			663, HBPL		689, GABI		
Pressure, kilobars		5.1, ALHB		5.1, ALHB		5.5, ALHB		5.1, GASP-Si			4.3, ALHB		5.9, GASP-Si		

Table 1 Compositions of Minerals used for Thermobarometry															
Map Number		39		40			41		42		43		44		
Field Number		JT89-16		179-NB205B			176-40		176-39		176-30		176-18		
Rock Unit		SP		SE			SP		SP		SP		SP		
Reference		1, 2		1			1		1		1		1		
Mineral		HB	PL	GA	BI	PL	HB	PL	HB	PL	HB	PL	HB	PL	
Wt% Oxide	SiO2	43.2	59.0	38.3	35.5	51.8	43.0	59.0	44.0	59.9	44.08	59.7	43.8	60.5	
	TiO2	1.20			3.03		0.83		0.72		0.75		0.84		
	Al2O3	13.0	25.3	21.0	17.9	28.5	11.1	24.8	10.4	24.7	10.2	24.3	10.7	24.5	
	FeO	18.0		30.6	15.2	0.01	18.3	0.03	17.5	0.04	17.3	0.13	17.3	0.14	
	MnO	0.43		0.84	0.01		0.53		0.41		0.49		0.44		
	MgO	8.69		6.27	11.8		10.1		11.0		11.4		11.0		
	CaO	11.4	7.03	1.79		12.2	11.4	6.23	11.6	6.20	11.6	6.06	11.5	5.95	
	Na2O	1.41	7.59		0.28	4.64	1.53	7.98	1.41	7.96	1.46	8.11	1.59	8.03	
	K2O	0.66	0.13		9.47	0.06	0.97	0.25	1.12	0.28	1.02	0.32	1.08	0.24	
	Total	98.0	99.0	98.7	93.2	97.2	97.8	98.3	98.2	98.0	98.3	98.6	98.3	99.3	
Cations		Si	6.40	2.66	3.04	5.43	2.42	6.39	2.67	6.49	2.68	6.47	2.70	6.45	2.71
	Ti	0.13				0.349		0.09		0.08		0.08		0.09	
	Al	2.27	1.34	1.96	3.23	1.57	1.94	1.33	1.81	1.32	1.76	1.29	1.86	1.29	
	Fe3	0.52					0.84		0.78		0.87		0.77		
	Fe2	1.71		2.03	1.95		1.43	0.001	1.38	0.002	1.26	0.005	1.36	0.005	
	Mn	0.05		0.056	0.001		0.07		0.05		0.06		0.05		
	Mg	1.92		0.742	2.69		2.24		2.42		2.49		2.41		
	Ca	1.81	0.339	0.152		0.611	1.81	0.303	1.83	0.302	1.82	0.293	1.81	0.285	
	Na	0.40	0.663		0.083	0.419	0.44	0.701	0.40	0.702	0.42	0.711	0.45	0.697	
	K	0.12	0.007		1.85	0.004	0.18	0.014	0.21	0.016	0.19	0.018	0.20	0.014	
Temperature °C		684, HBPL		730, GABI			738, HBPL		729, HBPL		750, HBPL		735, HBPL		
Pressure, kilobars		7.7, ALHB		6.1, GASP-Si			5.2, ALHB		4.8, ALHB		4.2, ALHB		4.9, ALHB		

Table 1 Compositions of Minerals used for Thermobarometry															
Map Number	45		46		47		48		49			50			
Field Number	176-15		164-350		164-347		164-280		164-203C			164-283			
Rock Unit	SP		SP		SP		SP		SE			SE			
Reference	1		1		1		1,2		2			1			
Mineral	HB	PL	HB	PL	HB	PL	HB	PL	GA	BI	PL	GA	BI	MU	PL
Wt% Oxide SiO ₂	42.3	60.9	44.2	61.1	43.6	58.4	42.4	59.9				36.7	35.3	47.5	59.9
TiO ₂	0.94		1.11		0.89		1.22					0.06	1.68	0.16	
Al ₂ O ₃	11.3	23.6	10.5	24.0	10.9	24.6	11.2	24.1				20.5	18.0	32.4	26.3
FeO	19.7	0.07	19.2		17.1	0.04	19.6	0.01				31.4	21.6	2.28	0.11
MnO	0.06		0.58		0.42		0.40					4.23	0.07		
MgO	8.50		9.22		11.1		8.87					1.70	8.72	1.81	
CaO	11.4	5.02	11.2	5.54	11.5	6.05	11.7	5.23				5.24			7.82
Na ₂ O	1.42	8.67	1.58	8.27	1.58	8.03	1.44	8.65					0.01	0.32	7.51
K ₂ O	1.46	0.17	0.79	0.29	1.08	0.24	1.37	0.13					8.94	10.4	0.05
Total	97.1	98.4	98.4	99.2	98.2	97.3	98.2	97.9				99.8	94.3	94.9	101.6
Cations Si	6.43	2.75	6.55	2.74	6.42	2.68	6.38	2.72	3.00	5.90		2.98	5.48	6.37	2.63
Ti	0.11		0.12		0.10		0.14			0.22			0.196	0.02	
Al	2.02	1.25	1.83	1.27	1.89	1.33	1.98	1.29	2.00	3.75		1.97	3.29	5.12	1.36
Fe ₃	0.48		0.65		0.79		0.54								
Fe ₂	2.02	0.003	1.73		1.31	0.002	1.93		2.19	2.34		2.13	2.80	0.256	0.004
Mn	0.01		0.07		0.05		0.05		0.15			0.291	0.009		
Mg	1.92		2.04		2.43		1.99		0.52			0.206	2.02	0.362	
Ca	1.86	0.243	1.78	0.266	1.81	0.297	1.88	0.254	0.32		0.31	0.456			0.368
Na	0.42	0.758	0.45	0.718	0.45	0.713	0.42	0.761		0.08	0.71		0.003	0.083	0.640
K	0.28	0.010	0.15	0.017	0.20	0.014	0.26	0.008		1.90			1.77	1.78	0.003
Temperature °C	682, HBPL		696, HBPL		736, HBPL		715, HBPL		620, GABI			494, GABI			
Pressure, kilobars	6.5, ALHB		5.5, ALHB		5.1, ALHB		5.8, ALHB		5.6, GASP-Ky			5.4, GAMI			

Notes for Table 1.

References:

1 = This study, 2 = Brown and Walker (1993), 3 = Brown and Burmester (1991), 4 = Bennett (1989), 5 = Reamsbottom (1974)

Rock unit abbreviations:

SE = Settler Schist, SL = Slollicum unit, SP= Scuzzy pluton, UP = Urquhart pluton.

Mineral Abreviations:

BI = biotite, GA = garnet HB = hornblende, MU = muscovite, PL = plagioclase.

Cations:

Based on charge balance (cation charge = garnet 24, mica 44, plagioclase 16, hornblende 46). Fe partitioned into ferrous and ferric states for amphibole only, based on charge balance and $(\text{Fe}+\text{Mg}+\text{Mn}+\text{Ti}+\text{Al}+\text{Si}) = 13$.

Temperature calculation:

HBPL = hornblende-plagioclase; calibration of Holland and Blundy (1994). GABI = garnet-biotite; calibration of Berman (1991); garnet solution model of Berman (1990); biotite solution model of McMullen and others (1991).

Pressure calculation:

ALHB = Al-in-hornblende; calibration of Anderson and Smith (1995). GASP-Si = garnet-quartz-plagioclase-sillimanite; GASP-Ky = garnet-quartz-plagioclase-kyanite; GAMI = garnet-quartz-biotite-muscovite-plagioclase; calibration of Berman (1991); garnet and biotite solution models as above; plagioclase solution model of Fuhrman and Lindsley (1988).

DR TABLE 2. U-Pb isotopic data and apparent ages.

Fraction-Size ^a (μ m)	Wt (mg)	Concentration ^b		Isotopic composition ^c			Apparent Ages (Ma) ^d			Th-corrected Ages (Ma) ^e		
		U	Pb*	$\frac{^{206}\text{Pb}}{^{204}\text{Pb}}$	$\frac{^{206}\text{Pb}}{^{207}\text{Pb}}$	$\frac{^{206}\text{Pb}}{^{208}\text{Pb}}$	$\frac{^{206}\text{Pb}^*}{^{238}\text{U}}$	$\frac{^{207}\text{Pb}^*}{^{235}\text{U}}$	$\frac{^{207}\text{Pb}^*}{^{206}\text{Pb}^*}$	$\frac{^{206}\text{Pb}^*}{^{238}\text{U}}$	$\frac{^{207}\text{Pb}^*}{^{206}\text{Pb}^*}$	
Sample 1. Fir Creek Pluton (# 179-NB16; lat 50°03.00'N, long 121°47.64'W)												
a	45-63	0.04	221	4.6	1794	17.360	7.766	154.8	155.7 \pm 0.4	170	154.9 \pm 0.3	169 \pm 3
b	63-80	0.7	239	5.8	10,363	19.720	9.596	155.6	156.0 \pm 0.3	162	155.6 \pm 0.3	161 \pm 1
c	125-145	1.2	227	5.5	7094	19.494	9.840	155.5	155.7 \pm 0.3	159	155.6 \pm 0.3	157 \pm 1
d	125-145A	0.7	147	3.6	5923	19.343	8.850	157.2	157.2 \pm 0.3	158	157.2 \pm 0.3	157 \pm 1
e	145-350A	0.4	193	4.7	6997	19.486	8.864	157.3	157.4 \pm 0.3	159	157.4 \pm 0.3	157 \pm 1
Sample 2. Settler Creek Pluton (# 179-MD25; lat 49°32.23'N, long 121°36.32'W)												
a	45-63	0.5	489	7.1	14,537	20.409	13.423	96.6	96.7 \pm 0.2	99	96.7 \pm 0.2	97 \pm 1
b	63-80A	0.9	278	4.1	23,038	20.515	12.392	97.1	97.4 \pm 0.2	105	97.2 \pm 0.2	103 \pm 1
c	80-100A	0.9	227	3.3	7041	19.961	11.781	97.0	97.1 \pm 0.2	100	97.0 \pm 0.2	98 \pm 2
d	80-100A	0.3	350	5.2	14,588	20.350	11.165	97.5	97.8 \pm 0.2	106	97.5 \pm 0.2	104 \pm 2
Sample 3. Hut Creek Pluton (# 179-CB22; lat 49°33.35'N, long 121°42.07'W)												
a	45-63	0.6	275	4.0	6767	19.953	10.571	94.2	94.3 \pm 0.2	97	94.3 \pm 0.2	95 \pm 2
b	63-80	0.4	199	2.8	3503	19.165	11.330	94.4	94.6 \pm 0.2	99	94.5 \pm 0.2	96 \pm 2
c	80-100A	0.5	171	2.4	9346	20.188	13.347	94.5	94.6 \pm 0.2	98	94.6 \pm 0.2	96 \pm 3
d	100-350A	0.4	185	2.7	4245	19.451	9.659	94.7	94.7 \pm 0.2	97	94.8 \pm 0.2	95 \pm 2
Sample 4. Hornet Creek Pluton (# 179-KS1; lat 49°38.58'N, long 121°47.00'W)												
a	63-80	0.8	179	2.6	2292	18.232	12.879	98.3	99.1 \pm 0.2	120	98.3 \pm 0.2	118 \pm 3
b	80-100	0.7	191	2.8	2332	18.185	13.046	99.0	100.3 \pm 0.3	133	99.1 \pm 0.2	131 \pm 4
c	100-350	0.2	164	2.5	1136	16.045	8.248	98.1	100.8 \pm 0.3	167	98.1 \pm 0.2	165 \pm 5
Partial Dissolution Results:												
		% U										
L1		2.4%	3	0.05	185	7.595	3.959	98.7	108.2 \pm 1.0	322	98.8 \pm 0.3	321 \pm 20
L2		51.0%	70	1.0	2955	18.670	15.207	98.2	99.4 \pm 0.3	128	98.3 \pm 0.3	127 \pm 2
L3		32.4%	44	0.7	9471	20.062	12.659	97.8	98.5 \pm 0.3	114	97.9 \pm 0.3	113 \pm 2
R		14.1%	19	0.3	3573	19.158	11.494	98.2	98.4 \pm 0.3	104	98.2 \pm 0.5	103 \pm 3
T	100-350	0.9	151	2.2				98.1	99.2 \pm 0.3	125	98.2 \pm 0.3	124 \pm 2
Sample 5. Breakenridge Pluton (# 180-GN; lat 49°37.60'N, long 121°50.36'W)												
a	63-80	0.6	148	2.4	1753	17.679	7.623	103.7	103.9 \pm 0.3	108	103.8 \pm 0.2	106 \pm 4
b	63-80	0.6	136	2.2	1461	17.158	7.405	103.7	103.9 \pm 0.3	110	103.8 \pm 0.2	108 \pm 4
c	80-100	0.7	130	2.1	1659	17.407	7.770	104.6	105.6 \pm 0.3	128	104.7 \pm 0.2	126 \pm 3
d	100-350	0.2	101	1.7	990	15.582	6.900	106.9	109.4 \pm 0.3	165	106.9 \pm 0.2	164 \pm 5
Sample 6. Urquhart Pluton (Rim) (#179-NB54; lat 49°43.42'N, long 121°42.07'W)												
a	45-63	0.6	449	5.9	4493	19.455	16.152	88.4	89.0 \pm 0.2	106	88.5 \pm 0.2	103 \pm 2
b	100-125	0.3	332	4.4	3735	19.197	14.532	89.5	90.1 \pm 0.2	107	89.5 \pm 0.2	105 \pm 2
c	145-350A	0.5	419	5.5	5024	19.630	14.654	88.0	88.4 \pm 0.2	100	88.1 \pm 0.2	98 \pm 2

Partial Dissolution Results:

	% U											
L1	26.3%	199	2.6	1897	17.946	14.680	88.3	88.6 ± 0.3	97	88.4 ± 0.3	96 ± 3	
L2	22.1%	167	2.1	2300	18.312	13.917	89.2	90.0 ± 0.3	110	89.3 ± 0.3	108 ± 3	
L3	33.1%	250	3.4	16,211	20.413	15.467	91.7	92.1 ± 0.3	103	91.7 ± 0.3	102 ± 2	
R	18.5%	140	2.0	22,184	20.590	14.232	92.3	92.3 ± 0.3	95	92.3 ± 0.3	93 ± 2	
T	145-350	2.2	344	4.6			90.4	90.8 ± 0.3	102	90.4 ± 0.3	100 ± 2	

Sample 7. Urquhart Pluton (Core) (#179-NB56; lat 49°39.81'N, long 121°42.07'W)

a	63-80	0.2	92	1.3	1011	15.904	8.028	90.8	91.8 ± 0.4	118	90.9 ± 0.2	116 ± 8
b	125-350	0.3	75	1.0	755	14.558	7.120	90.9	93.5 ± 0.5	160	90.9 ± 0.2	158 ± 11
c	125-350A	0.4	69	1.0	2082	18.113	9.468	91.0	91.6 ± 0.3	108	91.1 ± 0.2	106 ± 7

Partial Dissolution Results:

	% U											
L1	0.1%	0.3	0.002	28	1.734	0.655						
L2	2.0%	5	0.07	217	8.244	3.483	84.4	95.2 ± 0.8	376	84.4 ± 0.3	374 ± 17	
L3	15.6%	42	0.6	1019	15.786	8.817	91.1	93.1 ± 0.4	144	91.2 ± 0.3	143 ± 6	
L4	54.8%	146	2.0	11,010	20.259	11.374	91.2	91.6 ± 0.3	101	91.3 ± 0.3	99 ± 2	
R	27.6%	74	1.0	9850	20.251	10.612	91.1	91.2 ± 0.3	94	91.2 ± 0.3	93 ± 2	
T	125-350	3.8	70	1.0			91.0	91.7 ± 0.3	111	91.0 ± 0.3	110 ± 2	

Sample 8. Scuzzy Pluton (SW Rim) (# 179NB-18; lat 49°49.05'N, long 121°53.57'W)

a	63-80	0.8	295	3.8	8774	20.107	16.469	86.0	86.5 ± 0.2	102	86.0 ± 0.2	100 ± 1
b	80-100	0.3	258	3.4	5603	19.745	14.548	87.8	88.3 ± 0.2	100	87.9 ± 0.2	98 ± 3
c	100-350	0.8	339	4.3	13,008	20.337	18.432	86.3	86.8 ± 0.2	101	86.3 ± 0.2	99 ± 1

Partial Dissolution Results:

	% U											
L1	9.2%	53	0.6	1165	16.228	19.357	79.8	82.0 ± 0.3	148	79.8 ± 0.2	147 ± 6	
L2	87.2%	502	6.6	20,665	20.581	18.880	89.7	89.9 ± 0.3	93	89.8 ± 0.3	92 ± 2	
R	3.6%	21	0.3	3190	18.947	14.759	97.9	98.3 ± 0.3	109	98.0 ± 0.3	107 ± 4	
T	100-350	2.7	213	2.8			89.1	89.5 ± 0.3	99	89.2 ± 0.3	97 ± 2	

Sample 9. Scuzzy Pluton (NE Rim) (# 175-409; lat 50°03.00'N, long 121°47.64'W)

a	63-80	0.8	334	4.3	12,238	20.322	13.607	86.3	86.8 ± 0.2	100	86.4 ± 0.2	97 ± 1
b	80-100	0.8	377	4.9	12,765	20.336	13.638	86.7	87.2 ± 0.2	100	86.8 ± 0.2	98 ± 2
c	100-350	0.3	428	5.6	6535	19.911	12.470	86.9	87.3 ± 0.2	98	87.0 ± 0.2	96 ± 2

Partial Dissolution Results:

	% U											
L1	22.8%	83	1.0	3059	18.650	14.832	84.8	86.7 ± 0.3	139	84.9 ± 0.3	137 ± 5	
L2	75.4%	276	3.6	20,493	20.577	15.018	87.4	87.6 ± 0.3	93	87.4 ± 0.3	92 ± 2	
R	1.8%	7	0.1	1056	16.099	9.111	97.2	97.8 ± 0.4	112	97.2 ± 0.3	111 ± 5	
T	100-350	1.5	366	4.8			87.0	87.6 ± 0.3	104	87.0 ± 0.3	103 ± 2	

Sample 10. Scuzzy Pluton (Core) (#179-NB53; lat 49°51.53'N, long 121°44.29'W)

a	63-80	0.7	348	4.5	21,495	19.967	17.907	87.8	90.6 ± 0.2	167	87.8 ± 0.2	165 ± 2
b	80-100	0.7	411	5.2	15,353	19.819	19.387	85.8	88.8 ± 0.2	172	85.9 ± 0.2	169 ± 3
c	100-350	0.4	334	4.4	8604	18.823	18.713	89.3	95.7 ± 0.2	260	89.4 ± 0.2	258 ± 2

Partial Dissolution Results:

	% U											
La1	14.1%	69	0.8	2735	18.493	15.874	83.7	85.4 ± 0.4	134	83.8 ± 0.3	132 ± 7	
La2	84.1%	409	5.2	26,977	20.246	21.105	86.8	88.7 ± 0.3	141	86.9 ± 0.3	139 ± 1	
Ra	1.7%	8	0.2	2053	17.310	14.761	175.8	178.9 ± 0.6	225	175.5 ± 0.5	225 ± 4	
Ta	100-350	1.0	324	4.2			87.9	89.9 ± 0.3	143	88.0 ± 0.3	141 ± 2	
Lb1	6.1%	12	0.15	2629	18.725	18.470	87.7	87.8 ± 0.3	91	87.8 ± 0.3	90 ± 3	
Lb2	68.5%	131	1.62	20,561	20.439	20.599	84.2	85.1 ± 0.3	110	84.3 ± 0.3	108 ± 2	
Lb3	24.0%	46	0.58	9938	19.695	19.107	86.0	88.7 ± 0.3	162	86.0 ± 0.3	161 ± 2	
Rb	1.3%	3	0.04	451	12.086	7.551	100.5	105.0 ± 0.4	208	100.5 ± 0.3	207 ± 6	
Tb	80-350	0.6	347	4.3			85.1	86.4 ± 0.3	123	85.1 ± 0.3	121 ± 2	

Sample 11. Scuzzy Pegmatite (# 179-NB52; lat 49°43.05'N, long 121°50.90'W)

a	45-100	0.1	77	1.0	1890	17.981	23.515	90.6	90.7 ± 0.3	93	90.7 ± 0.2	91 ± 5
b	80-100	0.3	95	1.3	2654	18.381	23.029	93.1	94.9 ± 0.2	142	93.2 ± 0.2	140 ± 2
c	70-150	0.1	99	1.4	859	15.105	9.533	97.0	99.2 ± 0.3	153	97.0 ± 0.2	151 ± 6
d	80-350	0.2	104	1.3	1607	17.448	11.495	85.5	86.3 ± 0.2	108	85.6 ± 0.2	106 ± 2

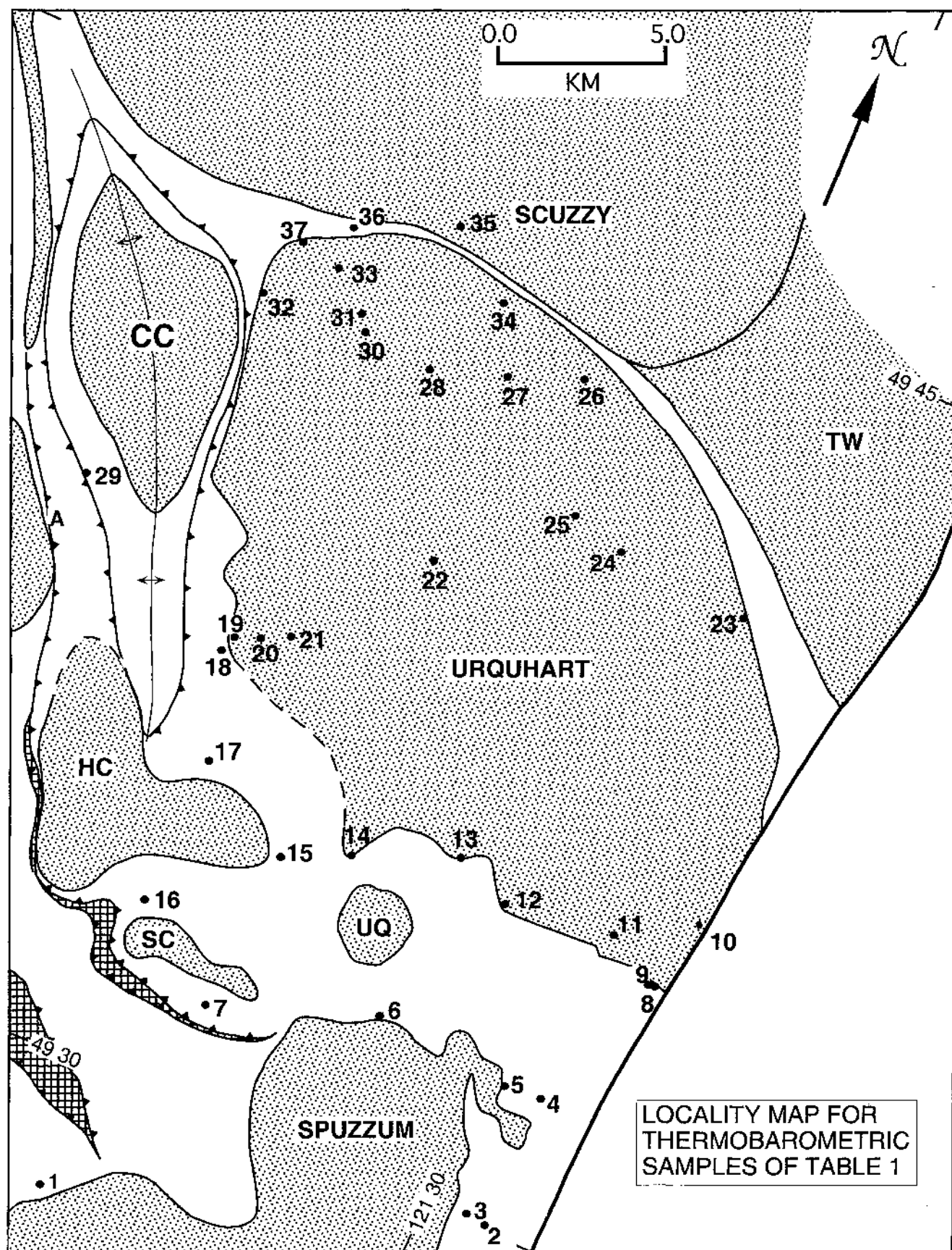
^a a, b, etc. designate conventional fractions; A designates conventional fractions abraded to 30 to 60% of original diameter; L1, L2, etc. designate leachate steps; R designates digestion of final residue; T designates mathematically recombined steps and residue. Dissolution schedule for 3-step experiments: 1 = 24 hours at 150°C; 2 = 24 hours at 210°C. For 4-step experiments: 1 = 24 hours at 80°C; 2 = 24 hours at 150°C; 3 = 24 hours at 200°C. For 5-step experiments: 1 = 24 hours at 80°C; 2 = 24 hours at 150°C; 3 = 24 hours at 200°C; 4 = 6 hours at 245°C. All conventional fractions and residues were dissolved in 60 hours at 245°C. All zircon fractions are non-magnetic on Frantz magnetic separator at 1.8 amps, 15° forward slope, and side slope of 4°: sample3; 3°: samples 8, 11; 2°: all others.

^b Pb* is radiogenic Pb and U expressed as ppm for conventional analyses and mathematically recombined partial dissolution totals. For partial dissolution steps, Pb and U expressed as nanograms and % of total U.

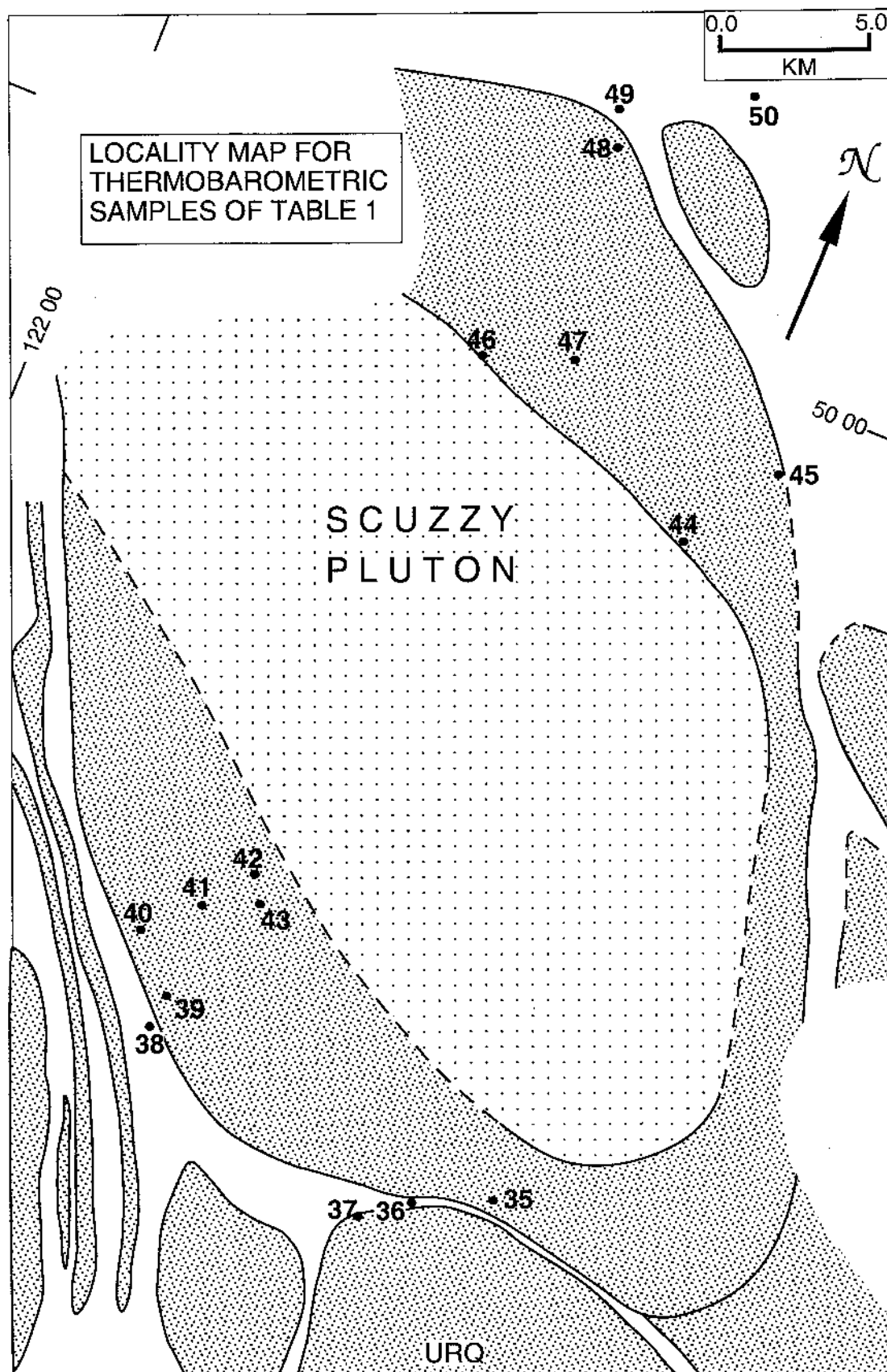
^c Reported ratios corrected for fractionation ($0.125 \pm 0.038\%/AMU$) and spike Pb. Ratios used in age calculation were adjusted for 10 to 20 pg of blank Pb with isotopic composition of $^{206}Pb/^{204}Pb = 18.6$, $^{207}Pb/^{204}Pb = 15.5$, and $^{208}Pb/^{204}Pb = 38.4$, 2 pg of blank U, $0.25 \pm 0.049\%/AMU$ fractionation for UO_2 , and initial common Pb with isotopic composition approximated from Stacey and Kramers (1975) and assigned uncertainty of 0.1 to initial $^{207}Pb/^{204}Pb$.

^d Uncertainties reported as 2 sigma. Decay constants: $^{238}U = 1.5513 \text{ E-10}$, $^{235}U = 9.8485 \text{ E-10}$; $^{238}U/^{235}U = 137.88$.

^e See procedure description for discussion of applied Th corrections.

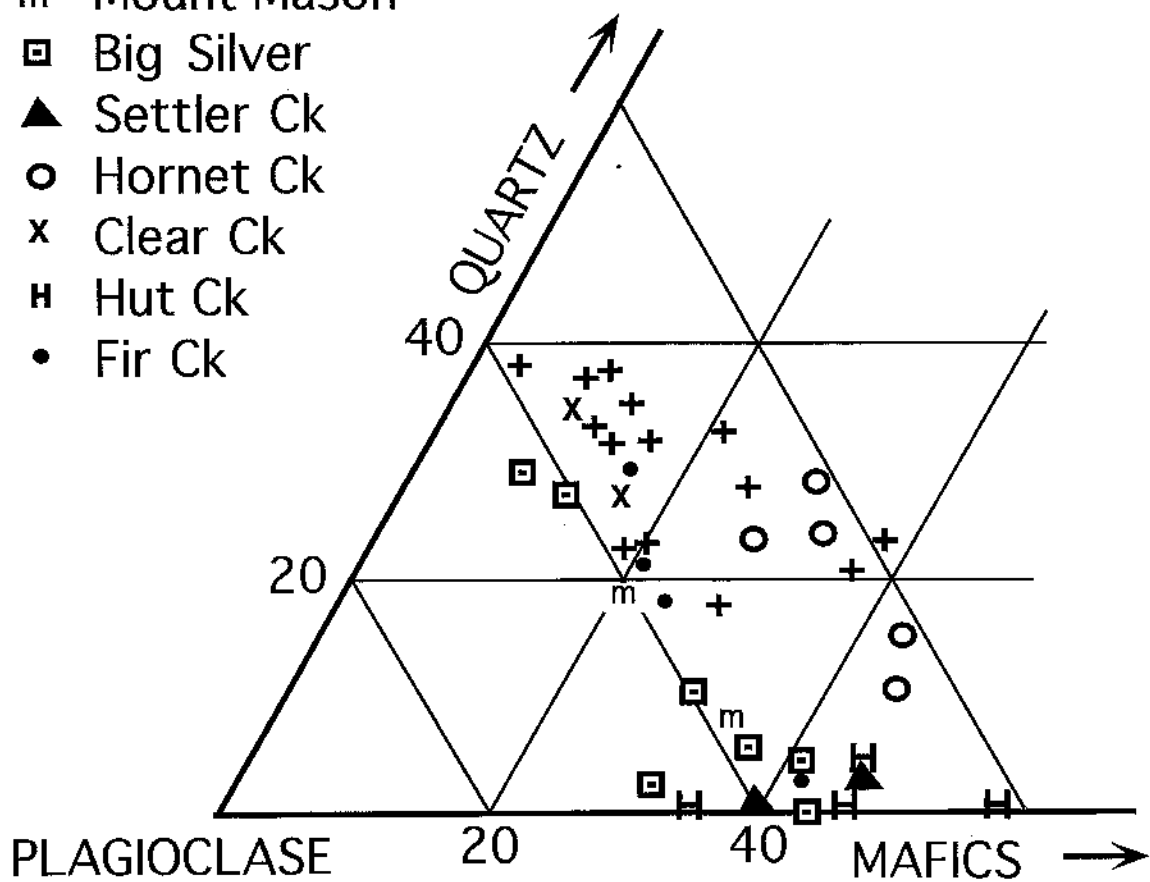


DR Fig. 1A

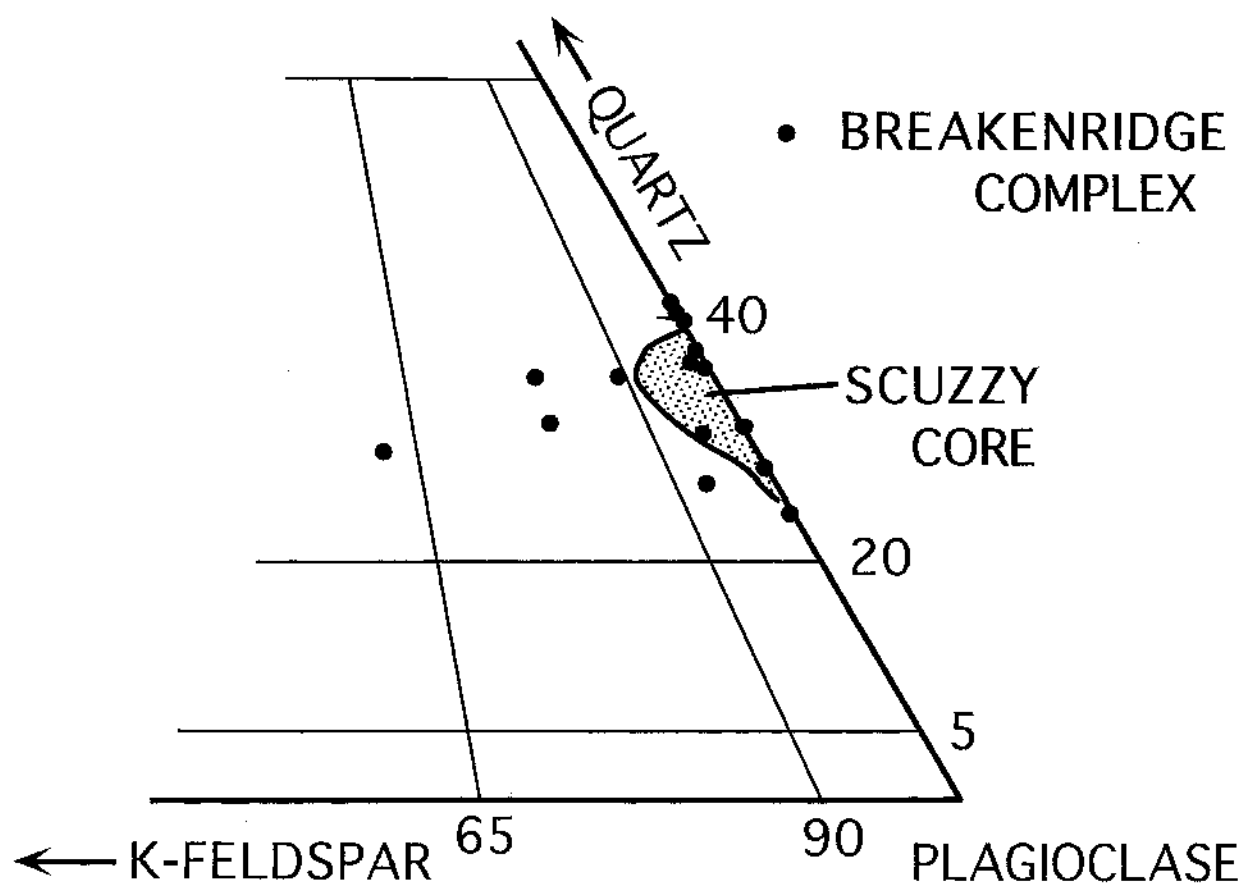


DR Fig. 1B

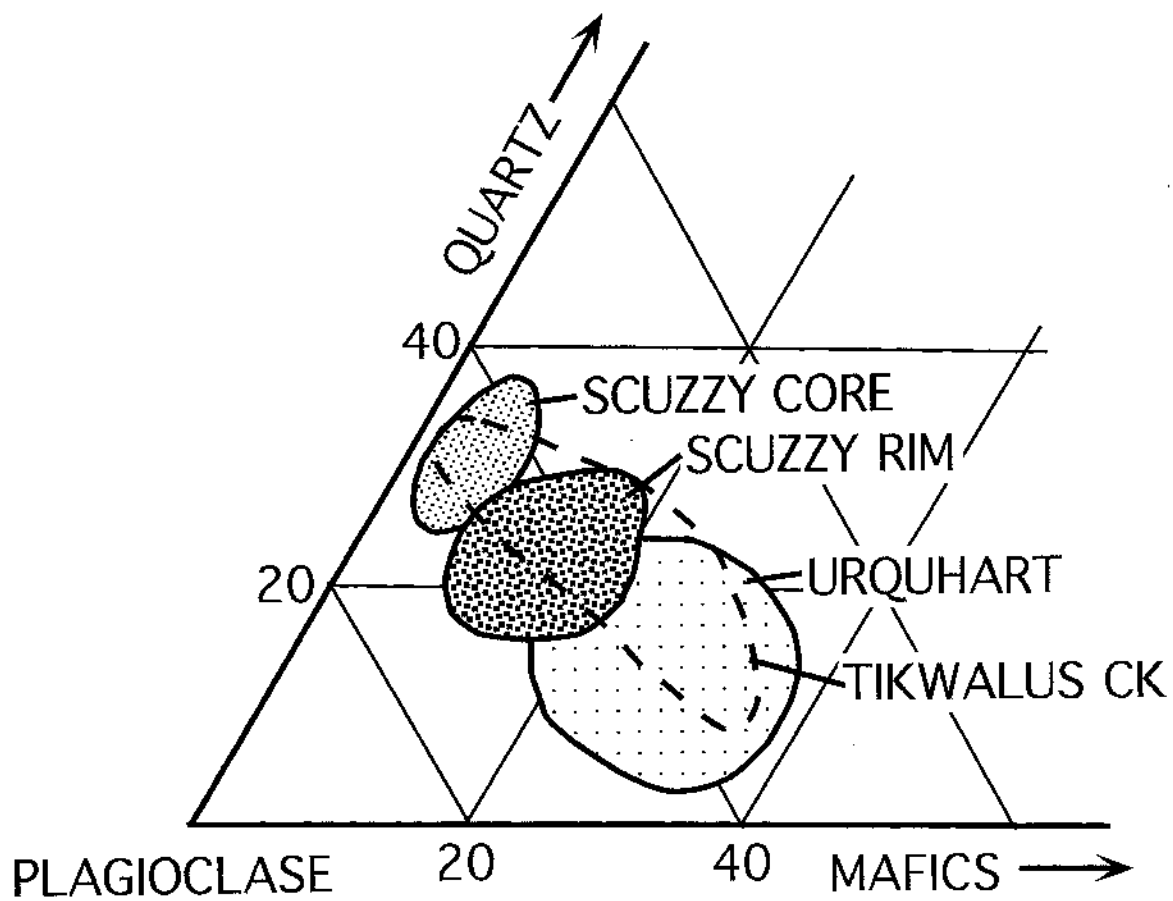
- + Breakenridge Cplx
- m Mount Mason
- ▣ Big Silver
- ▲ Settler Ck
- Hornet Ck
- x Clear Ck
- H Hut Ck
- Fir Ck



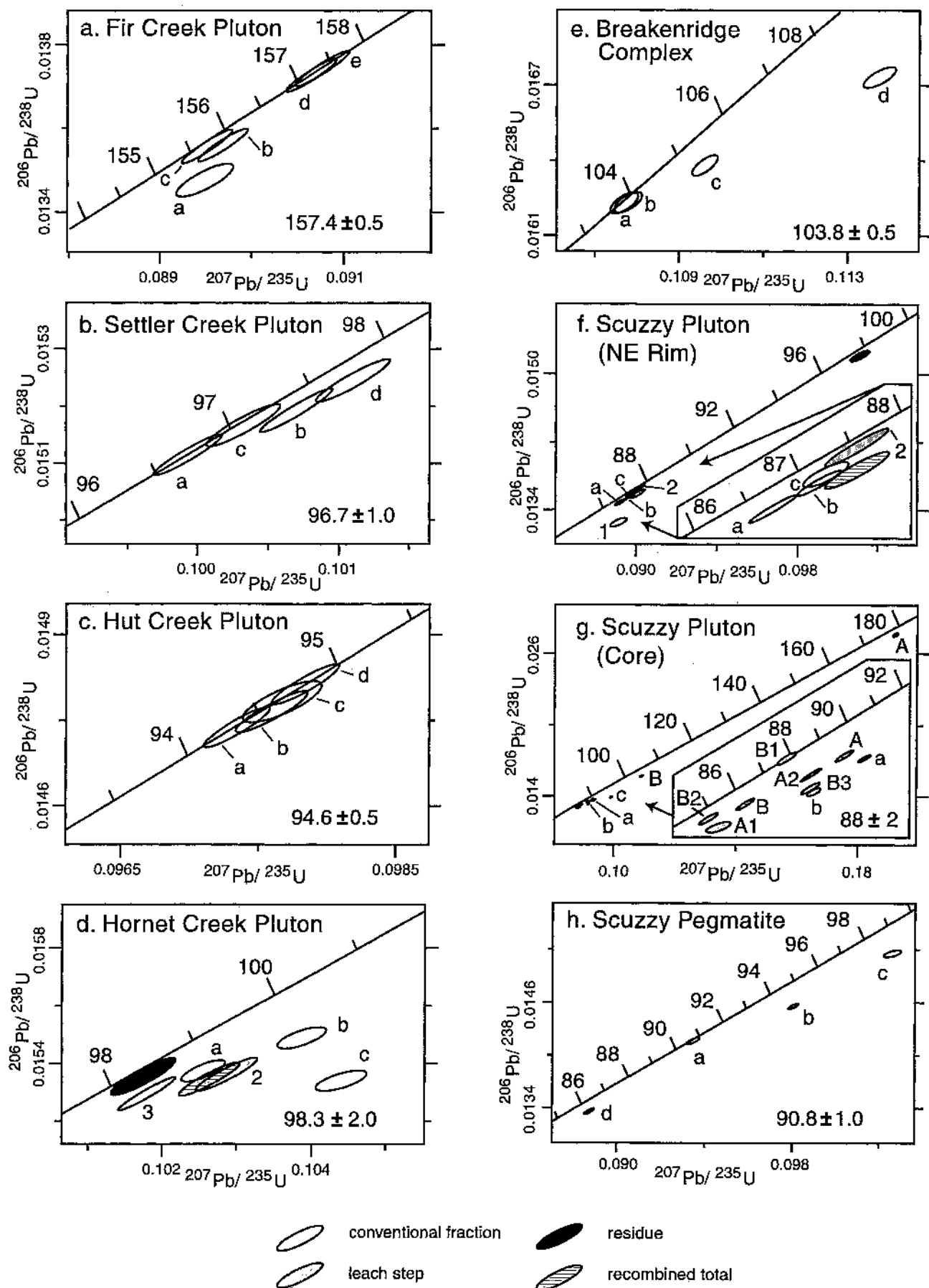
DR Fig. 2A



DR Fig. 2B



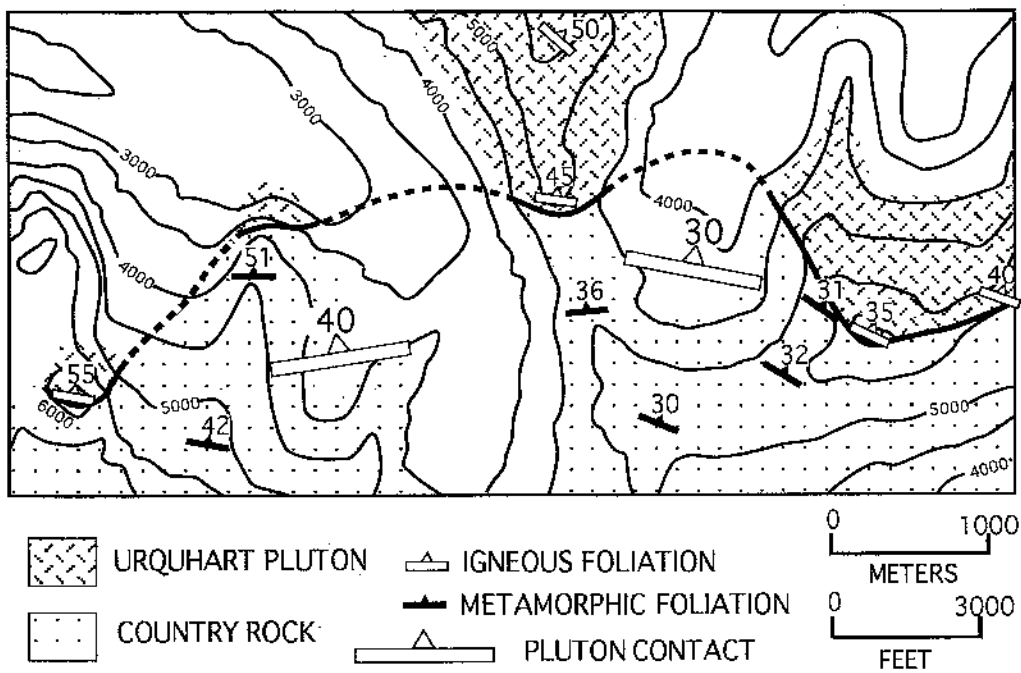
DR Fig. 2C



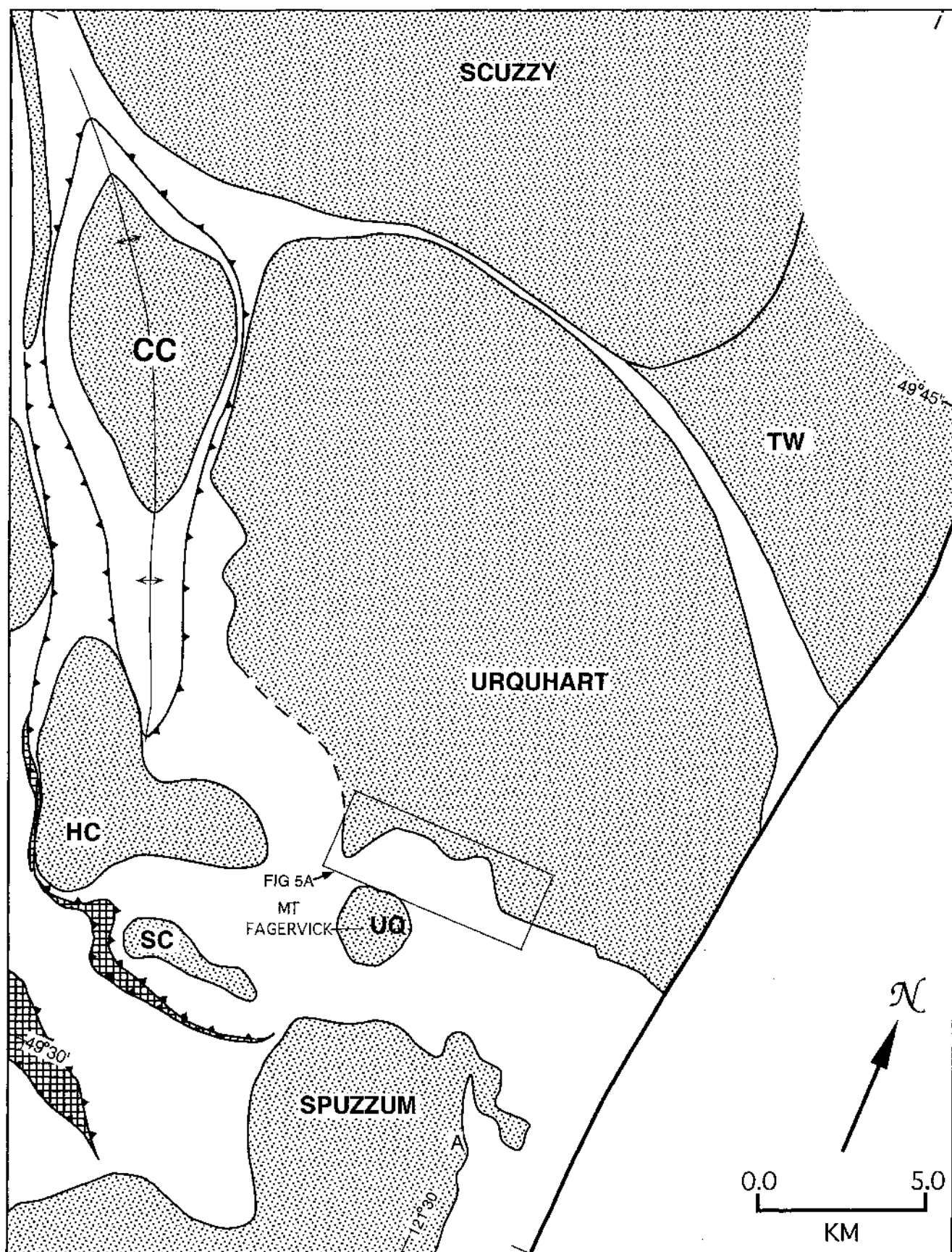
DR Fig. 3



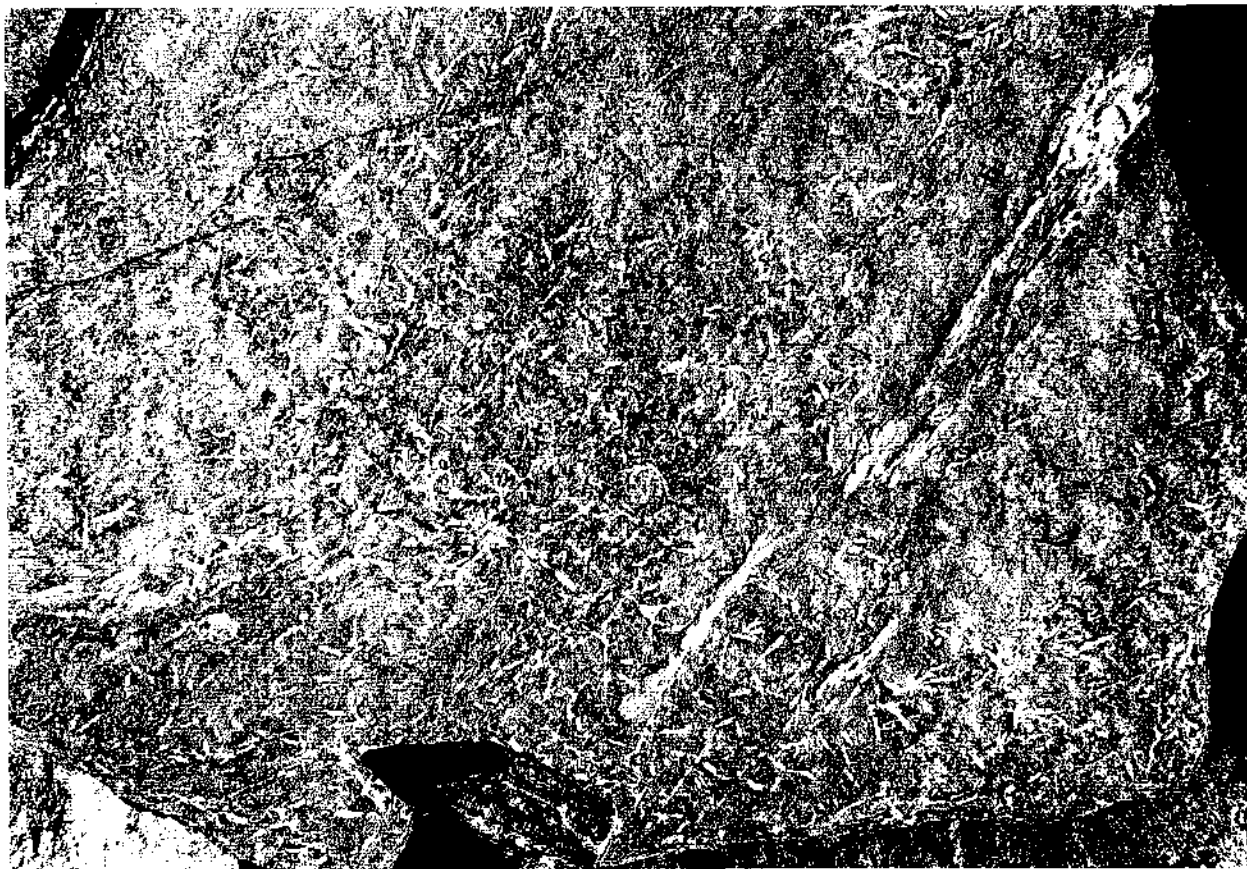
DR Fig. 4



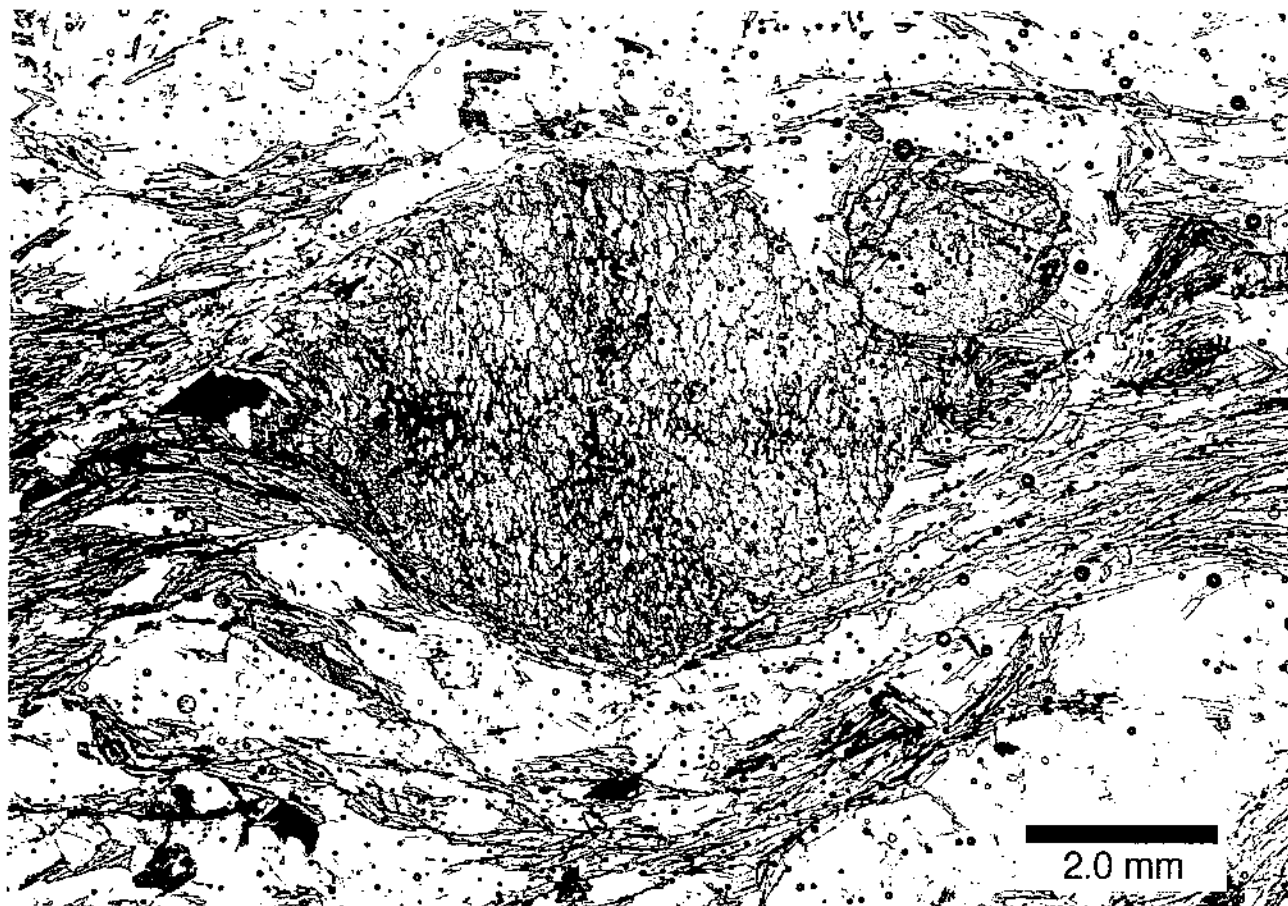
DR Fig. 5A



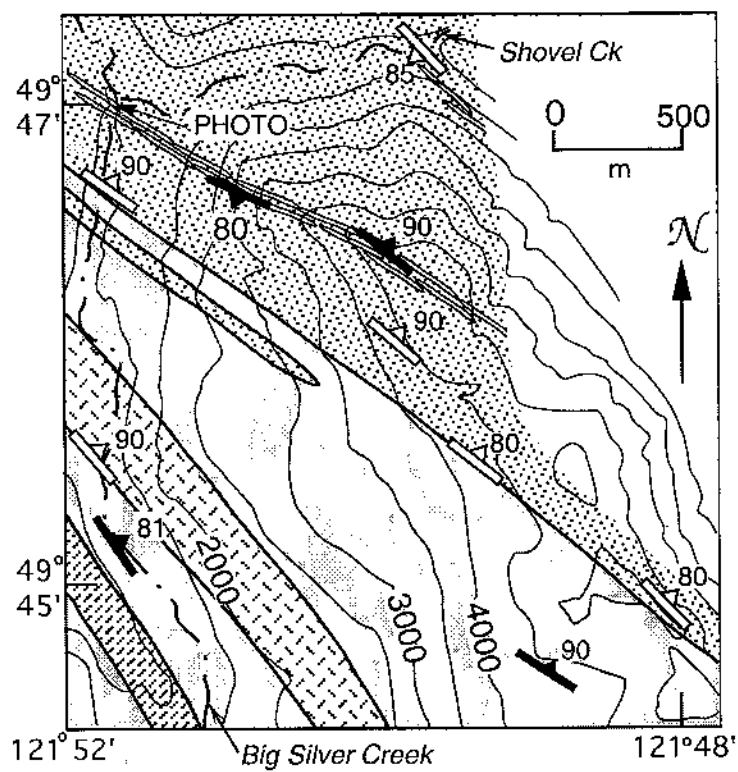
DR Fig. 5B



DR Fig. 6A



DR Fig. 6B



DR Fig. 7A

